Measurements in a Separation Bubble on an Airfoil Using Laser Velocimetry

Edward J. Fitzgerald* and Thomas J. Mueller†
University of Notre Dame, Notre Dame, Indiana

An experimental investigation was conducted to measure the reverse flow within the transitional separation bubble that forms on an airfoil at low Reynolds numbers. Measurements were used to determine the effect of the reverse flow on integrated boundary-layer parameters often used to model the bubble. Velocity profile data were obtained on an NACA 66_3-018 airfoil at angle of attack of 12 deg and a chord Reynolds number of 1.4×10^5 using laser Doppler and single-sensor hot-wire anemometry. Trends in displacement, momentum, and energy thickness growth as well as shape-factor variation with chordwise position were unaffected by reverse flow; however, significant errors in the magnitudes of the thicknesses and shape factors were realized by not accounting for local flow direction. The dividing streamline correlation proposed by Schmidt was evaluated and modified. A new correlation was proposed based on zero velocity position since the Schmidt correlations fail in the turbulent portion of the bubble. A two-parameter profile model gave better agreement than the Stewartson reverse-flow solutions with measured profiles. The poor agreement of the Stewartson profiles was attributed to the assumption of a power law external velocity distribution used to derive the Falkner-Skan equation.

Nomenclature

c = airfoil chord
f = Falkner-Skan similarity variable, $f' = U/U_{ext}$
H_{12} = shape factor, δ_1/δ_2
H_{32} = shape factor, δ_3/δ_2
h = distance between surface and separated shear layer in Green's profiles
ℓ = shear layer thickness in Green's two-parameter velocity profiles
P = parameter defining reverse-flow magnitude in Green's profiles
Q = net mass flux across a velocity profile
R_c = chord Reynolds number, $U_\infty c/\nu$
s/c = nondimensionalized airfoil surface arc length
U = local mean (tangential) velocity
U_{ext} = mean external velocity
x = surface distance from origin of boundary layer (Falkner-Skan equation)
x/c = nondimensional distance along chord
y = distance normal to airfoil surface
y_D = dividing streamline height
y_{ext} = height at which $U/U_{ext} = 0.99$
y_0 = zero streamline height
α = airfoil angle of attack
β = measure of favorable pressure gradient in Falkner-Skan equation
$\Delta y = y_{ext} - y_D$
δ_1 = boundary-layer displacement thickness, $\int_0^\delta (1 - U/U_{ext})dy$
δ_2 = boundary-layer momentum thickness, $\int_0^\delta (U/U_{ext})(1 - U/U_{ext})dy$
δ_3 = boundary-layer energy thickness, $\int_0^\delta (U/U_{ext})[1 - (U/U_{ext})^2]dy$
η = Falkner-Skan similarity variable
ν = kinematic viscosity

Subscripts

ext = external to boundary layer
∞ = freestream condition

Received July 8, 1988; revision received July 3, 1989. Copyright © 1989 by T. J. Mueller. Published by the American Institute of Aeronautics and Astronautics, Inc., with permission.

*Graduate Research Assistant, Department of Aerospace and Mechanical Engineering. Member AIAA.
†Roth-Gibson Professor, Department of Aerospace and Mechanical Engineering. Associate Fellow AIAA.

Introduction

THE advancements in aerospace materials, electronics, and control systems technologies over the past 20 years have expanded the realm of feasible aerospace flight vehicles. With these new technologies, aircraft power and size requirements have decreased and human pilots are not always necessary. High-altitude remotely piloted vehicles (RPV's) as well as mini-RPV's, sailplanes, ultralight aircraft, and even human-powered aircraft such as the Gossamer Albatross[1] and the Daedalus[2] are now a reality. What these aircraft all have in common is that they all operate at low chord Reynolds numbers.

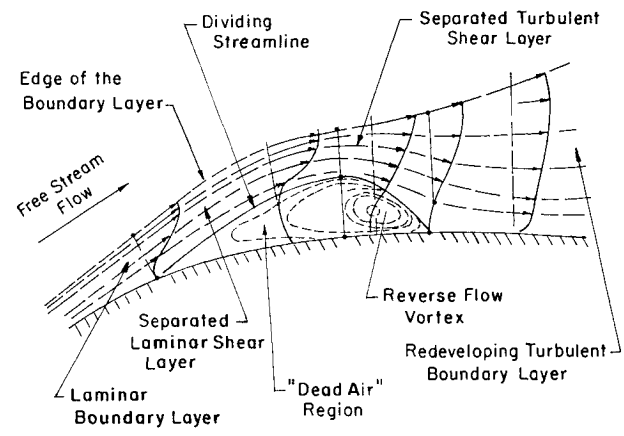

Fig. 1 Flow in the vicinity of a transitional separation bubble.[3]

The term "low Reynolds number" usually refers to R_c below 1×10^6, especially those less than 5×10^5. At these Reynolds numbers, the laminar boundary layer is stable enough to separate as a laminar free shear layer when it encounters an adverse pressure gradient rather than undergoing an attached transition process. The separated shear layer then transitions to turbulent flow. If sufficient energy can be entrained from the external flow, the now turbulent shear layer may reattach to form a transitional separation bubble, shown schematically in Fig. 1. Bubble size is dependent on several factors including freestream turbulence levels, airfoil surface roughness and angle of attack, and chord Reynolds number. Separation-bubble formation is generally undesirable; the locally separated flow degrades airfoil performance even when the bubble is only a few percent of the chord in length. In addition, small changes in freestream conditions or angle of attack can cause a short bubble to "burst" so that it covers a large percentage of the chord or stalls the airfoil.

Needless to say, modeling and predicting the characteristics of the separation bubble are difficult. Eppler and Somers[1] have developed a low-speed airfoil design code, but the code can only predict whether laminar separation will occur; it does not model the bubble itself. Researchers have used various methods to account for separation bubbles and their effect on airfoil performance. Semiempirical methods have been developed by Horton[3] for prediction of bubble bursting and by van Ingen and Boermans[4] for airfoil performance calculations. Both of these methods use semiempirical relations to calculate the parameters which define the bubble (e.g., separation, transition, and reattachment points). More theoretical methods of accounting for the effect of a separation bubble on airfoil performance include the viscous-inviscid interaction techniques of Kwon and Pletcher[5] and of Drela.[2] These techniques calculate the external flow using inviscid theory and the boundary-layer displacement thickness using viscous (typically integral) relations; the solutions are iterated to match the velocities at the viscous-inviscid interface.

Although these and other bubble-calculation schemes have been tested for Reynolds numbers above 1×10^6, the shortage of experimental boundary-layer data at Reynolds numbers below 5×10^5 hindered their validation in this regime. To fill this gap, O'Meara[6] made extensive hot-wire anemometry measurements of boundary-layer velocity profiles and spectra on a NACA 66_3-018 airfoil at Reynolds numbers between 5×10^4 and 2×10^5. He supported this data by taking static pressure distribution measurements for each case. Brendel[7] conducted similar tests on a Wortmann FX63-137 airfoil.

The difficulty with O'Meara's and Brendel's velocity profile data is that they were obtained with a single-sensor hot-wire anemometer. Thus, local flow direction could not be determined. From several analytical reverse-flow profile families, Schmidt[8] developed a dividing streamline correlation to allow correction of the boundary-layer parameters used to describe the bubble. Mangalam and co-workers[9] avoided this difficulty by making their measurements using a three-component laser Doppler velocimetry (LDV) system. These experiments, however, were made at $R_c = 2.1 \times 10^6$, well outside the low Reynolds number regime. The purpose of the present research was to measure the magnitude and direction of the flow within the separation bubble and to determine the effect of the direction of the flow within the separation bubble and to determine the effect of the directional ambiguity on experimentally derived parameters used in separation-bubble models. To this end, velocity profiles were measured on the NACA 66_3-018 airfoil using laser Doppler velocimetry for the $R_c = 1.4 \times 10^5$, $\alpha = 12$ deg case. This case was chosen because it had been extensively studied by both O'Meara and Schmidt. In addition, single-sensor hot-wire measurements were also repeated for this case to guarantee that any differences between the LDV data and O'Meara's hot-wire data was not because of changes in tunnel facilities. The data was then analyzed and compared to several empirical, analytical, and semiempirical criteria used to predict and model separation-bubble characteristics.

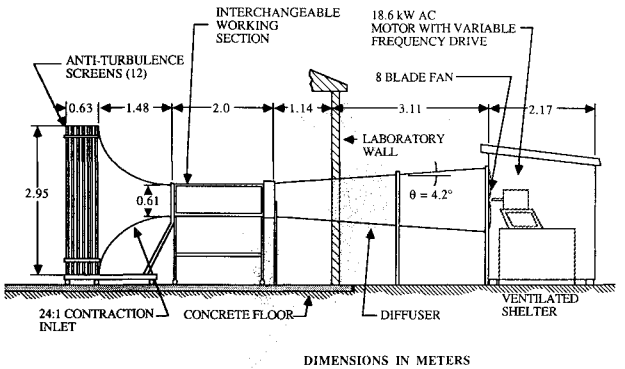

Fig. 2 Notre Dame Aerospace Laboratory subsonic wind tunnel.

Experimental Apparatus

All experiments were performed in the south subsonic low-speed wind tunnel at the University of Notre Dame. The tunnel is an indraft, nonreturn type and is shown in Fig. 2. The 24:1 contraction ratio inlet and 12 antiturbulence screens produce a low turbulence level in the test section, measured by a single-sensor hot-wire to be less than 0.08% for a 1-2500 Hz bandwidth.[10] Separate test sections were used for laser Doppler and hot-wire anemometry. Each test section was square in cross section, 0.61 m by 0.61 m, and 1.83 m long. To allow LDV measurements in forward-scatter mode, the first test section had three plate glass walls and a plexiglass back wall fitted with a holder for the airfoil sting.

The second test section was used for all hot-wire anemometry measurements. Computer-controlled linear traversers allowed vertical and chordwise movement of the hot-wire probe, and a (computer-controlled) rotary table was used to set the angular orientation of the probe with respect to the airfoil model. The traversal system had resolutions of 0.006 mm (0.00025 in.) in the chordwise direction, 0.013 mm (0.0005 in.) in the vertical direction, and 0.05 deg for sensor pitch control.

For both LDV and hot-wire experiments, a single NACA 66_3-018 airfoil model with a 249.5-mm chord and a 410-mm span was used. The epoxy model was painted flat black. Chordwise positions were marked on the upper surface of this model with white ink in a row offset 3.8 cm (1.5 in.) from midspan. These marks were used for chordwise positioning of the LDV's measuring control volume (the LDV "probe" formed by the crossed laser beams). The airfoil was mounted between two 61-cm square plexiglass sideplates to minimize end effects.

Single-component LDV measurements were made of the tangential velocity component using a 5-W argon ion laser, a signal conditioner/burst counter, a frequency shifter, and transmitting and receiving optics. Frequency shifts of 1 or 2 MHz were necessary to measure the reverse flow within the bubble. The entire system was mounted on a three-component traversing table. Each traverser had a resolution of 0.0254 mm (0.001 in.). To improve the signal-to-noise ratio, the LDV was operated in the forward-scatter mode. Since room dust did not provide adequate seeding in the separation-bubble region, smoke particles were introduced into the flow upstream of the wind-tunnel inlet. The seeding smoke was produced by vaporizing kerosene in a smoke generator designed by Brown.[11]

Hot-wire anemometry data was acquired using a constant-temperature anemometer and a single-wire boundary-layer probe. The hot-wire was calibrated against a pitot-static probe before each test. In order to study the fluctuating part of the anemometer signal better, the signal was decomposed into mean and fluctuating branches, and each branch was conditioned separately. For both the hot-wire and LDV experiments, DEC PDP-11 minicomputers and associated conversion hardware were used for acquisition and computational

reduction of data. More information on the experimental apparatus can be found in Ref. 12.

Results

Boundary-Layer Velocity Profiles

To investigate the effects of probe interference on hot-wire velocity profile data and to determine experimentally the magnitude of the reverse flow and its effect on the separation-bubble parameters, laser Doppler velocimeter measurements were made in the boundary layer for the $R_c = 1.4 \times 10^5$, $\alpha = 12$ deg case. These results are plotted with corresponding hot-wire data in Fig. 3. Since the LDV is capable of measuring reverse flows, the magnitude and direction of the velocity is apparent throughout each profile. Separation occurs near $x/c = 1\%$. With increasing x/c, the shear layer moves farther away from the wall, and the reverse flow, first measured at $x/c = 2\%$, increases in magnitude and extent. The recirculation zone reaches its maximum height at $x/c = 7\%$, which was designated as the transition point. Although transition is a gradual process that occurs over a finite length, most computational models characterize transition as the point where the computer program switches from laminar to turbulent boundary-layer relations to calculate the flow. Thus, instead of defining a transition length as suggested by Arena,[13] a transition point was designated. Downstream of transition, the shear layer moves closer to the airfoil surface as the turbulent shear layer entrains fluid from the external flow and decreases the extent of the reverse-flow region. Reattachment has occurred by $x/c = 13\%$. The recirculation zones are very clear in each of the velocity profiles. The agreement of the shear layer and external velocity distributions is good except for the profiles near transition at $x/c = 7\%$. These differences can be attributed to the hot-wire's inability to distinguish the tangential from the normal velocity component of the reverse-flow vortex.

The reverse flow within the separation bubble has a large effect on the integrated boundary-layer thicknesses and shape factors. The integrated-thickness development in the separation-bubble region is shown in Fig. 4. The displacement-thickness growth trends are independent of measurement technique. The local maxima in δ_1 for the hot-wire and LDV data occur at approximately the same chordwise position. The difference is in the magnitudes of δ_1. Both the hot-wire and LDV values of δ_1 grow at roughly the same rate after separation until $x/c = 5\%$. From this point aft, the reverse-flow vortex has a significant effect on the velocity profile shapes: the reverse tangential and the normal velocity components increase, magnifying the distortions inherent in the hot-wire measured velocity profile. The fuller profiles measured by the hot-wire cause the δ_1 growth rate to slow producing a local δ_1 maximum more than 23% lower than the corresponding LDV measurement. Schmidt found that hot-wire data could yield δ_1 values as much as 20% below the true values because of not taking into account flow direction.[8] The additional 35% difference in δ_1 in the bubble region may be attributed to Schmidt's assumption of a linear velocity profile. This assumed profile shape allowed Schmidt to observe error trends in separation-bubble parameters when flow direction is not taken into account, but actual error magnitudes would differ since the true profiles are not linear. After transition, δ_1 decreases with x/c at nearly the same rate for both hot-wire and LDV measurements because of the reduction in the height of the recirculation zone. The fact that a significant discrepancy in δ_1 still exists after reattachment at $x/c = 12\%$ is because of the unsteady nature of the reattachment process. The reattachment point was determined in these experiments from the mean velocity profile and other mean parameters. The instantaneous reattachment point varies significantly; instantaneous reverse flow was measured as far aft as $x/c = 15\%$. By $x/c = 25\%$, when reverse flow is no longer present, differences in δ_1 are within the uncertainty (<0.1 mm) caused by the uncertainty in the LDV measuring volume relative to the airfoil surface (± 0.2 mm).

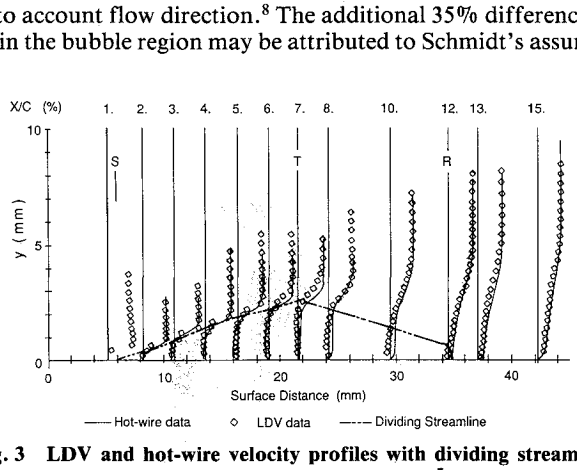

Fig. 3 LDV and hot-wire velocity profiles with dividing streamline directly calculated from LDV data ($R_c = 1.4 \times 10^5$; $\alpha = 12$ deg).

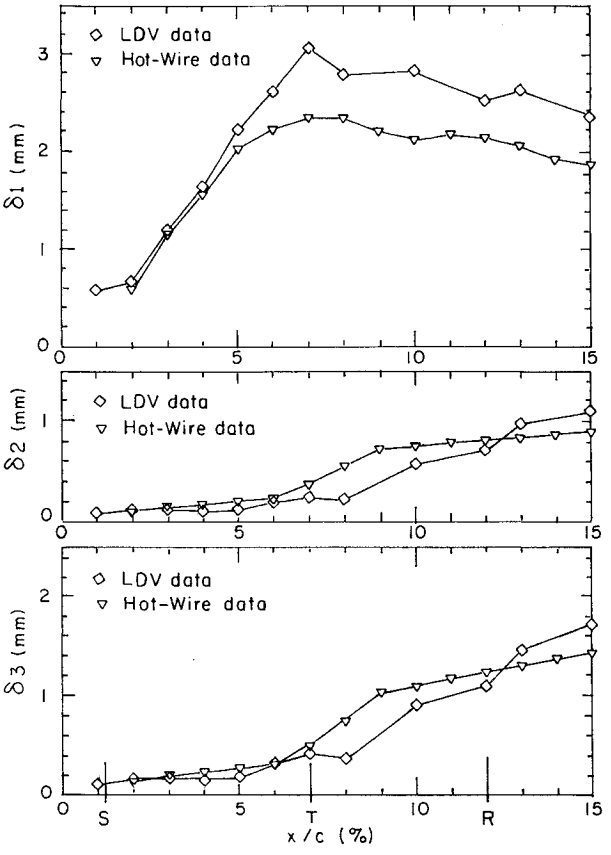

Fig. 4 Comparison of integrated boundary-layer parameters computed from hot-wire and LDV data ($R_c = 1.4 \times 10^5$; $\alpha = 12$ deg).

The hot-wire values for the momentum and energy thicknesses follow the same growth trends as the LDV values. The significant growth in δ_2 in the laminar portion of the bubble noted by Schmidt[8] from O'Meara's data is also seen in the LDV data where δ_2 nearly triples between separation and transition. As predicted by Schmidt,[8] δ_2 and δ_3 values are larger within the separation bubble when flow direction is not taken into account. Schmidt found that hot-wire data could yield δ_2 values with over 250% error and δ_3 values with over 200% error within the bubble. Although the differences in the hot-wire and LDV data follow the predicted trend, however, the discrepancies are less pronounced. The maximum error in the hot-wire momentum thickness is less than 140%. The errors in δ_2 and δ_3 measured by the hot-wire are usually less than 100% when compared to the LDV thicknesses. This better-than-expected agreement between the hot-wire and LDV values for these parameters may again be attributed to Schmidt's linear profile assumption. As would be expected, the agreement of the hot-wire and LDV data improves as the recirculation zone

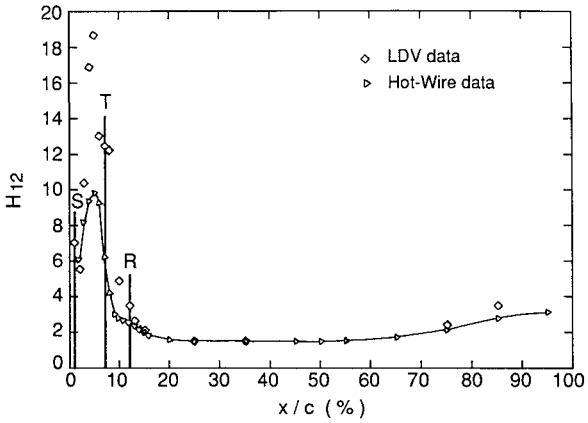

Fig. 5 Effect of reverse flow on H_{12} ($R_c = 1.4 \times 10^5$; $\alpha = 12$ deg).

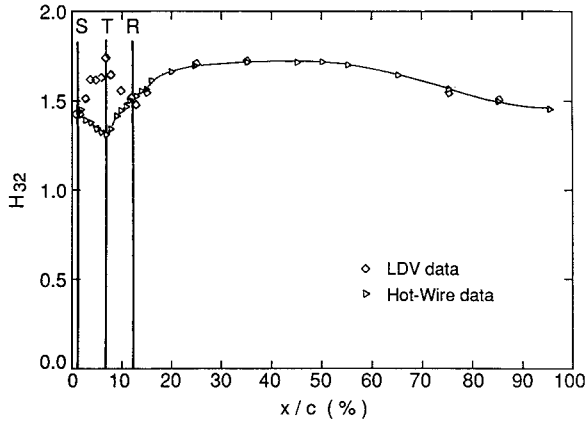

Fig. 6 Effect of reverse flow on H_{32} ($R_c = 1.4 \times 10^5$; $\alpha = 12$ deg).

decreases. The differences in δ_2 and δ_3 magnitude and growth rate immediately aft of reattachment are again because of differences in the mean velocity profiles caused by instantaneous reverse (and in the case of the hot-wire, normal) flow. When instantaneous reverse flow is no longer present, the discrepancy between the thicknesses is less than 10%.

Not unsurprisingly, the shape factors H_{12} and H_{32} exhibit similar phenomena. The variation of H_{12} and H_{32} with x/c for hot-wire and LDV data are shown in Figs. 5 and 6, respectively. As expected from Schmidt's findings, the hot-wire values for these parameters are smaller than the values from the LDV data. Again, although the trends in the hot-wire error are as expected, the magnitudes of these discrepancies differ from what Schmidt expected: hot-wire H_{12} errors are only -64% (Schmidt expected -80%), but hot-wire H_{32} errors are as high as -25% while Schmidt expected only -10%. As before, as the amount of reverse flow decreases, the agreement becomes better. The trends in H_{12} growth agree well. The only surprise comes in the H_{32} variation within the bubble. Mangalam and co-workers[9] observed the same H_{32} behavior demonstrated by the hot-wire data: H_{32} decreased with x/c after separation until transition occurred whereby it increased to an approximately constant value after reattachment. The H_{32} values calculated from the present LDV data, however, grow with x/c from separation to transition then decrease until reattachment. The energy thickness grows faster than the momentum thickness in the laminar portion of the bubble, but after transition the momentum-thickness growth rate increases more than the energy-thickness growth rate. The discrepancy in H_{32} behavior is not because of the measurement uncertainty in H_{32} (less than 10%). It should be mentioned that the LDV data of Mangalam et al.[9] was obtained on the underside of the leading edge of a supercritical airfoil at a chord Reynolds number of 2.1×10^6. Furthermore, Brendel[7] has shown that even in the same low Reynolds number range, the H_{32} trend from hot-wire measurements can vary radically depending on the location and length of the separation bubble. The difference between LDV and hot-wire results in separation bubbles requires more study.

Dividing Streamline

The net mass flux Q between the airfoil surface and the mean dividing streamline shown in Fig. 1 is zero; that is,

$$\int_0^{y_D} U \, dy = 0 \tag{1}$$

Thus, in a mean sense at least, this streamline encloses the pocket of recirculating fluid and defines the extent of the transitional separation bubble. Knowledge of the dividing streamline location removes the necessity of determining the velocity distribution within the recirculation zone in order to correctly determine displacement, momentum, and energy thicknesses and their related shape factors.[8] If the dividing streamline location were known for all cases, integrated thicknesses and shape fractors within the bubble could be determined from single-sensor hot-wire data. Since the LDV data took into account flow direction, the dividing streamline was calculated by direct integration of the velocity profiles. The resulting streamline for the $R_c = 1.4 \times 10^5$, $\alpha = 12$ deg case is plotted in terms of surface arc length (from the airfoil leading edgte) in Fig. 3 with the corresponding LDV and hot-wire velocity profiles. No relationship between y_D and the external velocity is readily apparent.

Surprisingly, the dividing streamline predicts a longer overall bubble than expected. The bubble reaches its maximum thickness at transition, approximately 7% x/c. After transition, the expected behavior of the turbulent shear layer is a quick reattachment over only a few percent of the chord, resulting in a turbulent portion of the bubble that is much shorter than the laminar section. What is suggested by a least-squares line fit of y_D downstream of transition is that reattachment occurs at $x/c = 13.5\%$. The result is a turbulent portion

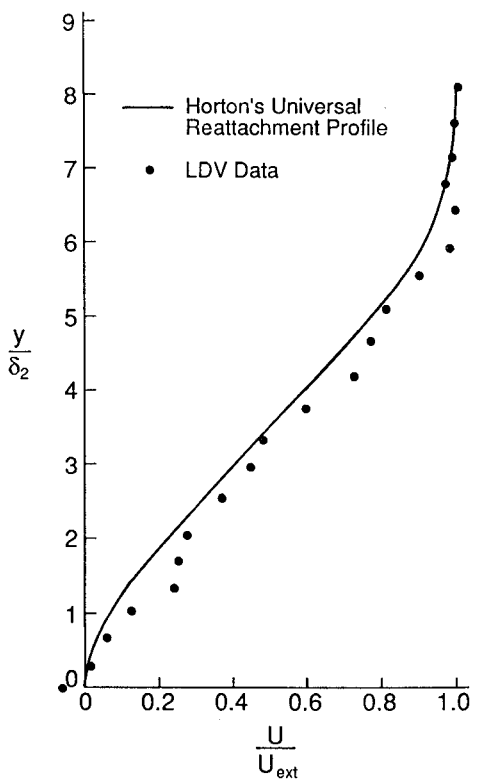

Fig. 7 Comparison of Horton's universal reattachment profile to LDV measurements at $x/c = 12\%$.

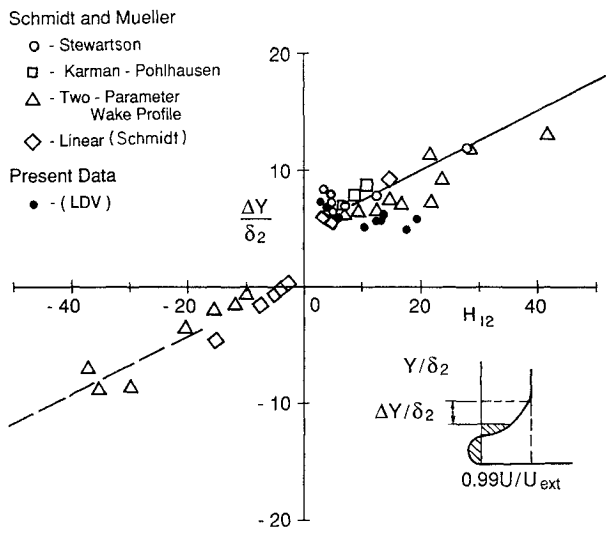

Fig. 8 Schmidt's dividing streamline correlation data and present LDV data.

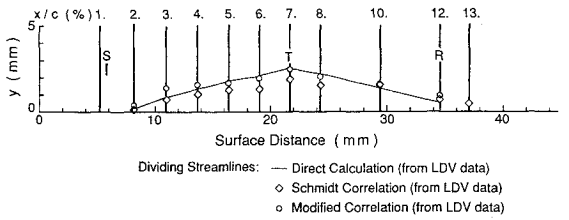

Fig. 9 Dividing streamline comparison: Streamlines calculated from LDV data ($R_c = 1.4 \times 10^5$; $\alpha = 12$ deg).

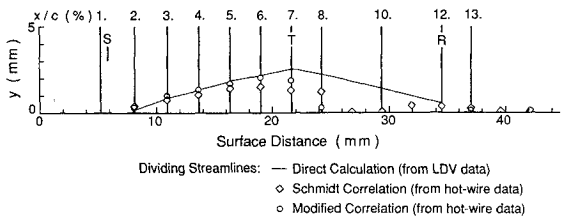

Fig. 10 Dividing streamline comparison: Streamlines calculated from hot-wire data ($R_c = 1.4 \times 10^5$; $\alpha = 12$ deg).

of the bubble of nearly the same length as the laminar portion. Horton found that the turbulent portion could reach 40% of the overall bubble length in some cases.[3] However, this extreme value still underestimates the turbulent length without providing an explanation for the discrepancy. Schmidt's lampblack flow visualization showed a turbulent portion of approximately 50% for this condition.[14] These discrepancies in the length of the turbulent portion may be because of the highly unsteady nature of the reattachment phenomenon. Instantaneous reverse flow was measured near the surface through $x/c = 15\%$. Whereas 72% of the velocities sampled near the wall at $x/c = 12\%$ were negative, by $x/c = 15\%$ only 4% of the samples near the wall were negative. The dividing streamline position may reflect this reverse-flow intermittancy. In addition, since only three profiles were measured downstream of transition, the apparent linear trajectory of the dividing streamline may be a product of too few points to define the streamline shape in the turbulent portion of the bubble adequately. For the purposes of this study, $x/c = 12\%$ was chosen as the mean reattachment point because this profile closely resembled the universal reattachment profile used in Horton's analysis[3] (see Fig. 7). In addition, mean profiles at x/c greater than 13% were attached, and this choice produced a turbulent portion of more classical length.

In order to correct O'Meara's hot-wire data, Schmidt developed a correlation based on the dividing streamline position relative to the edge of the boundary layer, $\Delta y/\delta_2 = (y_{ext} - y_D)/\delta_2$, with the velocity profile's shape factor H_{12} from several families of reverse-flow velocity profiles. Schmidt's data and his corresponding least-squares line fits are shown with the present LDV data in Fig. 8. When applied to either LDV or hot-wire data, the correlation was found to underpredict y_D by as much as 30% as shown in Figs. 9 and 10. From the plot in Fig. 8, it is clear why the underprediction occurred. Only three of the nine LDV data points fall on the line defining the correlation; the other six fall below the lower edge of the scatter of the data Schmidt used. Thus, with increasing H_{12}, the correlation diverges from the measured values. The LDV data show that the recirculation zone measured by the LDV takes up a much larger percentage of the velocity profile than any of the analytical profiles with a shape factor greater than six.

The LDV $\Delta y/\delta_2$ data suggest a different correlation: either a constant value for $\Delta y/\delta_2$ over an H_{12} range of 3-24 or a slight decrease in $\Delta y/\delta_2$ over this same range rather than the increase called for by the correlation. Even the analytical profiles give a relatively constant value for this H_{12} range. Schmidt[8] also noted this phenomenon but chose the two least-squares line fits in an attempt to maintain the generality of the correlation. It may be too much to expect a single correlation to hold over such a wide range of H_{12}. Because the H_{12} values—valid for separation bubbles—all fall between 3 and 24, a constant value for $\Delta y/\delta_2$ may be a good general correlation for this specific type of flowfield. To determine a suitable value for this constant, the analytical and experimental data within this H_{12} range were averaged yielding a constant $\Delta y/\delta_2 = 6.3$ for $3 \le H_{12} \le 24$.

Recalculating the dividing streamline for the LDV using the modified correlation produced much better results as shown in Fig. 9. The discrepancies which remain in the dividing streamlines shown in the figure are because of the assumption in the computer routine that the dividing streamline occurs at a data point. In the profiles at either end of the bubble, the experimental data points on either side of the dividing streamline happened to be far enough apart that when the routine matched expected and calculated values of $\Delta y/\delta_2$, the true y_D was skipped over and a greater value was chosen. This problem could be solved by refining the computer code. This example demonstrates that the modified correlation does work.

Similarly, good results were obtained when the modified correlation was applied to the hot-wire data as illustrated in Fig. 10. There is less overshoot or undershoot in the laminar portion of the bubble than was seen in the LDV (modified correlation) case because more points per profile were measured by the hot wire; consequently, the interval around the dividing streamline is smaller and less error is incurred in assuming y_D coincides with a data point. The good agreement continues until near transition where the correlation falls apart. Distortion of the velocity profile due to the single-sensor hot-wire's inability to differentiate even between tangential and normal velocity components causes excessive underestimation of H_{12}. These initial values of H_{12}, directly measured by the hot wire, are so far from the true values that the profiles appear to the routine to be attached, and thus the iterations are stopped long before y_D is reached. This is not too surprising since Horton[3] found that reattachment corresponded to a shape factor of 3.5. The initial values of H_{12} for the hot wire profiles downstream of transition ($x/c = 7\%$) are lower than 3.5 so the routine predicts attached profiles for $x/c > 8\%$. Because the normal component cannot be removed from the velocity profiles measured by the hot wire, correction of this data would be difficult. A good first estimate of the streamline position, perhaps assuming it corresponded to the zero velocity point y_0 in the profile above the airfoil surface, might allow

a better determination of y_D using the correlation. In any case, the dividing streamline correlation can be used to determine y_D in the laminar portion of the bubble.

Zero Streamline

It was observed when comparing the LDV and hot-wire velocity profiles that not only did the separated shear layers agree well (especially in the laminar portion of the bubble) but that the point of zero velocity in the LDV profiles exhibiting reverse flow could be approximated by the intersection of a straight-line fit of the points in the "shear layer" section of each hot-wire profile where the local velocity was between 31 and 95% of U_{ext}. By fitting data in this region of the shear layer, hot-wire rectification effects on profile shape were minimized. All hot-wire data measured above this intersection point in the profile under consideration could be assumed to be unaffected by reverse flow; data measured below the zero-velocity point had been rectified reverse flow. The attraction of determining the y_0 point in this way is that it can be obtained from the hot-wire data even in the turbulent portion of the bubble. Admittedly, the approximation is poorer near and aft of transition, but hot-wire profiles from this region of the bubble are significantly altered by the reverse tangential and the normal components of the recirculation vortex; characteristic features of the true (tangential) velocity profiles in this region are difficult to discern.

Since y_0 can be approximated from the hot-wire profiles, a relation between y_0 and y_D was also investigated. Such a relation would allow determination of the dividing streamline position. A relation between these two parameters was found from the LDV data by plotting y_D vs y_0 and doing a least-squares line fit as shown in Fig. 11. The equation for the line is

$$y_D = 0.0642 + (1.3198)y_0 \tag{2}$$

where y_D and y_0 are both in millimeters. The graph shows y_D to be directly proportional to y_0. Although Eq. (2) may only hold for these velocity profiles, the low scatter in the data is encouraging.

Analytical Profile Models: Stewartson Profiles

Since the ultimate goal of this research is to find a method for predicting and modeling transitional separation bubbles, the reverse-flow profiles obtained using laser velocimetry were compared with analytically derived reverse-flow profiles. One such family of profiles are solutions to the Falkner-Skan equation[15]:

$$f''' + ff'' + \beta(1 - f'^2) = 0 \tag{3}$$

Stewartson[16] showed that for $-0.19884 < \beta < 0$, two solutions exist for a given β. One of these solutions is a velocity profile

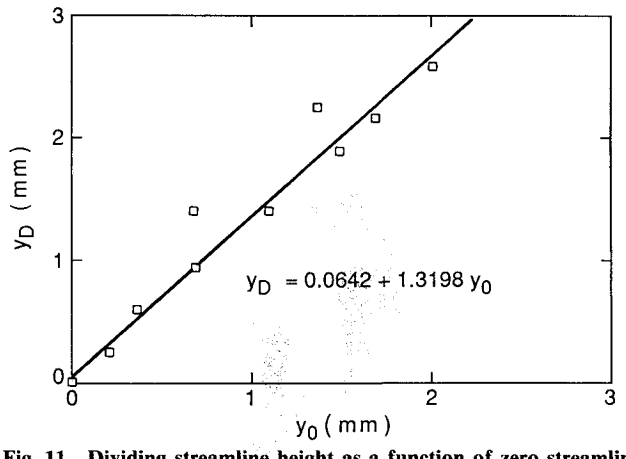

Fig. 11 Dividing streamline height as a function of zero streamline height ($R_c = 1.4 \times 10^5$; $\alpha = 12$ deg).

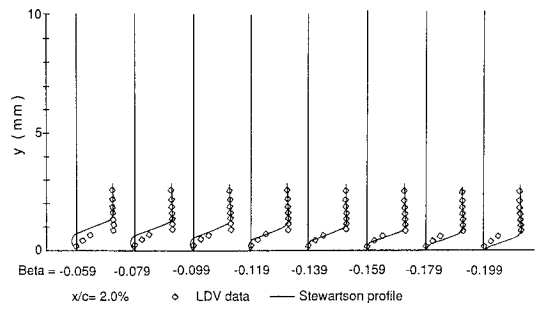

Fig. 12 Comparison of Stewartson velocity profiles to LDV profile at $x/c = 2\%$ ($R_c = 1.4 \times 10^5$; $\alpha = 12$ deg).

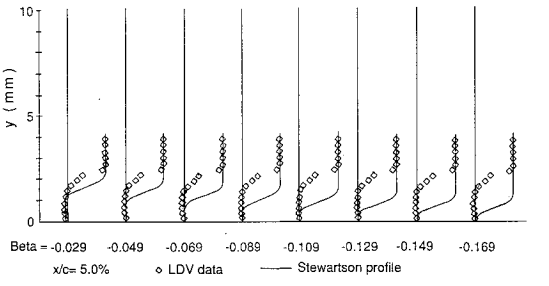

Fig. 13 Comparison of Stewartson velocity profiles to LDV profile at $x/c = 5\%$ ($R_c = 1.4 \times 10^5$; $\alpha = 12$ deg).

with reverse flow. Since some researchers, notably van Ingen and Boermans[4] as well as Vincent de Paul,[17] use these Stewartson solutions to the Falkner-Skan equation to model the velocity profiles within the separation bubble and make stability calculations, comparisons were made of the Stewartson profiles with those measured by the LDV.

Stewartson profiles were generated by integrating the Falkner-Skan Equation (3) using a fourth-order Runge-Kutta routine. The experimental slope at the wall measured in the $x/c = 2\%$ LDV velocity profile was used as an initial guess of the Stewartson profile slope at the wall $f''(0)$. This initial guess was then iterated until the $f'(\infty)$ conditions were matched. For each x/c, β was varied from -0.029 to -0.199 by steps of -0.01; $\beta = -0.029$ converged to the attached solution for the given β. Each Stewartson profile was then compared to the LDV profile. The representative cases of $x/c = 2\%$ for $-0.199 < \beta < -0.059$ and of $x/c = 5\%$ for $-0.169 < \beta < -0.029$ are shown in Figs. 12 and 13, respectively.

The Stewartson profiles resulting from the study have the shapes one might expect to find in a separation bubble. As is clear from the figures, however, the agreement between the calculated and measured profiles diminishes with increasing x/c. The best agreement occurs for the profiles near separation. At $x/c = 2\%$, shown in Fig. 12, Stewartson profiles $\beta = -0.139$ to -0.179 may adequately agree with the LDV profiles. As the measured separated region increases with increasing x/c, the disagreement between the calculated and measured velocity profile shapes becomes more clear. The Stewartson profiles consistently underpredict the height of the recirculation zone while overpredicting the magnitude of the reverse-flow velocities. For the β that best match the magnitude of the LDV profile's minimum velocity, the height of the recirculation zone may be off by a factor of four or more. If the heights of the reverse-flow regions can be matched ($x/c < 5\%$), the Stewartson profiles exhibit negative velocities twice those measured with the LDV. Note that even when the heights of the shear layers match, the velocity distributions (i.e., the "shapes of the shear layers") do not.

The poor agreement can probably be attributed to the variation in external velocity distribution over the airfoil surface. The Falkner-Skan equation assumes that U_{ext} varies as $x^{\beta/(2-\beta)}$, where x is surface position measured from the begin-

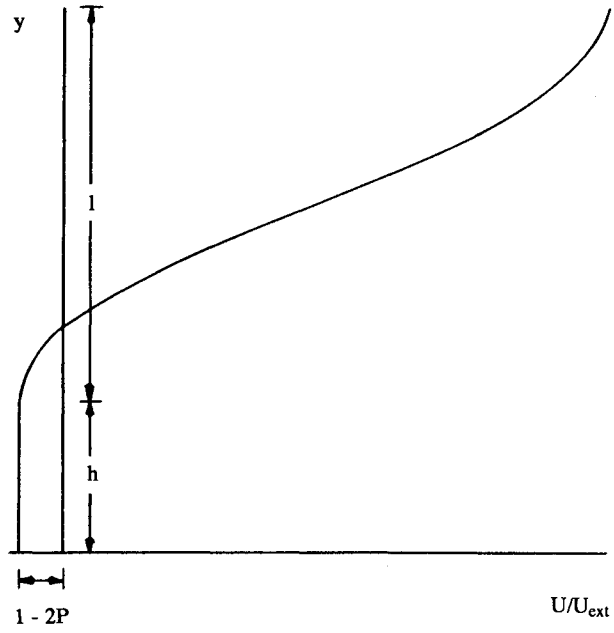

Fig. 14 Green's two-parameter model of a velocity profile in a turbulent wake.

ning of the boundary layer and β is a constant. The measured variation in external velocity can be satisfactorily represented by such a function from the airfoil suction peak to separation; downstream of separation, however, the measured velocity distribution diverges from the power law. Since the power law holds until near separation, the velocity profiles immediately downstream of separation agree fairly well, but the agreement diminishes downstream. The fact that the pressure gradient along the airfoil surface changes from favorable to adverse (i.e., β varies with surface position) between the airfoil stagnation and shear-layer separation points may also explain the differences noted in the shapes of the LDV and Stewartson profiles. It was found, however, that the variation of y_D as a function of y_0 for Stewartson profiles[4] agreed quite well with Eq. (2). This can be attributed to the fact that y_D is essentially an integral quantity and that the underpredicted recirculation height and the overpredicted reverse-flow velocities cancel. The Stewartson profiles would not appear to be a good approximation for the velocity profiles within the separation bubble formed on an airfoil, although some integral parameters derived from these profiles may be useful.

Analytical Profile Models: Green's Two-Parameter Profiles

In examining Schmidt's dividing streamline correlation, it was noted that one of the analytical profile families used in defining the correlation came closer to the values of $\Delta y/\delta_2$ measured by the LDV than the others in the shape factor range covered by the separation-bubble profiles. The two-parameter wake profile family of Green[18] remained relatively constant for H_{12} between 5 and 22 as well as producing the smallest values of $\Delta y/\delta_2$ over this range of any of the other analytical velocity profile families Schmidt considered. This profile family was therefore investigated as a candidate for modeling the profiles within the separation bubble.

Green's two-parameter velocity profile[18] was developed to model turbulent reattachment occurring in a wake region. In the flowfield Green modeled, profiles downstream of the reattachment point were represented by Cole's family of wake velocity profiles. Velocity profiles upstream of reattachment were represented by an area of constant velocity bounded by a (separated) shear layer. The resulting profile is shown in Fig. 14. These profiles are based on the parameter P from Cole's family and a second parameter h (often nondimensionalized by the shear layer thickness ℓ) which defines the distance between the surface (or in Green's case the wake centerline) and the shear layer. The velocity distribution for $0 \le y \le h$ is given by

$$\frac{U}{U_{\text{ext}}} = 1 - 2P \tag{4}$$

and for $h \le y \le (h + \ell)$ is given by

$$\frac{U}{U_{\text{ext}}} = 1 - P\left[1 + \cos\left(\pi \frac{y - h}{\ell}\right)\right] \tag{5}$$

Note that the defined "shear layer" (of length ℓ) extends below y_0 for these profiles.

In the present case, it was hoped that the two-parameter profile might be a suitable model for the separation-bubble velocity profiles. The simplicity of the profile itself allowed extreme flexibility when attempting to match it with experimentally determined velocity profiles and promised computational ease in any future separation-bubble calculation schemes used in airfoil design and performance-evaluation programs.

In order for the two-parameter profile model to be of use in a separation-bubble modeling or prediction routine, the variation of the parameters P and h/ℓ with surface position must be defined. To obtain such relations, the minimum and zero-velocity points of each experimental (LDV) profile were matched, and the variation of P and h/ℓ with surface arc length was noted. From this parameter-variation data, linear relations were defined which followed the data trends as shown

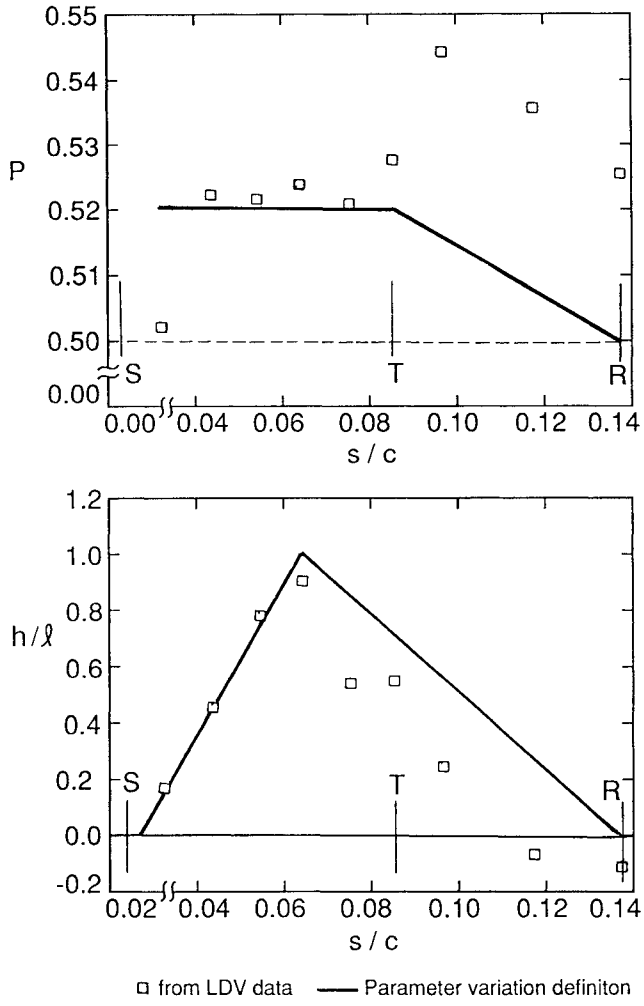

Fig. 15 Derivation of parameter-variation relations for Green's profile using LDV profile data ($R_c = 1.4 \times 10^5$; $\alpha = 12$ deg).

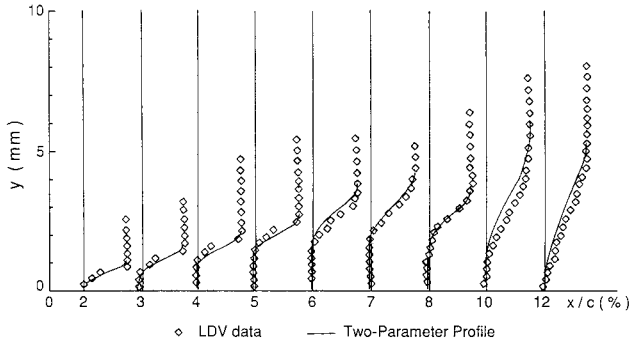

Fig. 16 Comparison of two-parameter velocity profiles to LDV measured profiles ($R_c = 1.4 \times 10^5$; $\alpha = 12$ deg).

in Fig. 15. Note that s/c is measured relative to the airfoil leading edge. The change in the h/ℓ variation trend 2.1% s/c (2% x/c) before transition can be attributed to the change in velocity profile character that accompany the transition process; with the approach of transition, the shear-layer thickness ℓ increases faster than the height h. The post-transition increase in P and the negative values of h/ℓ near reattachment show that the minimum and zero-velocity points of the experimental profile could not both be matched for these cases without one parameter (h/ℓ) becoming physically unrealistic; hence, the linear relations were defined for the turbulent portion of the bubble-to-force reattachment at the experimental reattachment point, $x/c = 12\%$ ($s/c = 0.0653$).

Considering the simplicity of the parameter-variation relations chosen, the agreement of the analytical and experimental profiles, shown in Fig. 16, is amazingly good. Not unexpectedly, the best agreement occurs for those profiles at $x/c \leq 5\%$ ($s/c = 0.0653$). It was in this portion of the bubble that the parameter variations were most well-behaved probably because of the orderliness of laminar flow. The worst agreement occurred at $x/c = 10$ and 12%. Even for these two profiles, however, the vertical shift of the analytical profile is not much more than the uncertainty associated with the vertical position of the first LDV data point in each profile.

Although more refined relations for P and h/ℓ variation might produce slightly better agreement for $x/c > 5\%$, the simple relations used in this analysis show the value that the two-parameter profile could have in a separation-bubble model. The main shortcoming of the two-parameter profile as applied in this study is that the P and h/ℓ variation just described has little analytical basis; each "analytical" profile is in effect a curve fit of experimental data. The values for the tested correlation are based on experimentally determined transition and reattachment points. Since these values change for every case, the universality of any of these relations is doubted. However, the worst agreement obtained with the two-parameter profile was better than the best obtained with the Stewartson family of profiles. In addition, the calculations necessary for computing Stewartson profiles are much more time-consuming than those used for Green's two-parameter family. The good agreement with experimental data, despite the simplicity of the empirical trends used to define parameter values, makes the two-parameter profile family appear to be a better model prospect for separation-bubble flow than the Stewartson family of profiles.

Conclusions

The objective of the present study was to determine the effect of the reverse flow within the transitional separation bubble on the bubble parameters that are used in various analytical models to predict and evaluate the influence of the separation bubble on airfoil performance. To this end, boundary-layer velocity profiles were measured using the LDV for the $R_c = 1.4 \times 10^5$, $\alpha = 12$ deg case. Once this data had been obtained, comparisons between data collected by different acquisition techniques and comparisons with analytical models were made.

As expected, good agreement between the LDV and hot-wire velocity profiles was found in the separated shear layer and attached turbulent boundary layer where reverse flow did not occur. The effect of the reverse flow on the displacement, momentum, and energy thicknesses was only to change the local magnitudes of the parameters; the same spatial growth trends observed in the hot-wire data were also observed in the LDV data. For instance, the significant growth in δ_2 noted by Schmidt in O'Meara's hot-wire data still occurred in the laminar portion of the bubble.

Errors incurred in integrated thicknesses by not accounting for flow direction were magnified in the shape factors H_{12} and H_{32}. Errors in H_{12} of over 65% of the true value were noted, but the hot-wire data followed the same trends as the LDV data. The H_{32} variation within the bubble from the LDV data followed the opposite trends observed in the hot-wire data. The energy-thickness growth over the laminar portion was greater than the momentum growth before transition; after transition, this trend reversed until reattachment occurred. This produced a local maximum in H_{32} at transition.

Direct calculation of the dividing streamline from the LDV data revealed that Schmidt's dividing streamline correlation underpredicted y_D. This underprediction was because of two factors. The shapes of the analytical profiles he used to define the correlation were different from the experimentally measured profile shapes. More importantly, the behavior of the correlation parameter for the separation bubble was changed by trying to extend the correlation over too large a range of H_{12}. By redefining the correlation over the H_{12} range applicable to separation bubbles, good agreement between the (modified) correlation and the directly calculated dividing streamline heights was realized in the laminar portion of the bubble. The distortion of the hot-wire profiles in the turbulent portion of the bubble because of the hot-wire's inability to distinguish between tangential and normal velocity components caused extreme underprediction of y_D. A y_D correlation based on another feature of the velocity profile is necessary in the turbulent portion of the bubble. Such a correlation based on y_0 was derived from the directly calculated LDV data. The applicability of the relation to other Reynolds number conditions has not yet been tested.

Although several researchers use the Stewartson family of velocity profiles to model separation-bubble profiles, comparison of these profiles to experimentally determined profiles produced poor agreement. A much simpler profile family, the two-parameter turbulent wake profile of Green, produced much better agreement with the experimental profiles. The agreement for profiles after separation to near reattachment was maintained even for very simple definitions of parameter variation with s/c. Although these relations were dependent on experimentally measured profiles, more universal relations can probably be derived. The overall simplicity of the Green profile family makes it very attractive for modeling the separation bubble using computer codes.

Acknowledgments

This research was supported by NASA Langley Research Center under Grant NSG-1419 and by the Department of Aerospace and Mechanical Engineering, University of Notre Dame.

References

[1]Mueller, T. J., "Low Reynolds Number Vehicles," AGARDograph No. 288, Feb. 1985.

[2]Drela, M., "Low Reynolds Number Airfoil Design for the M.I.T. Daedalus Prototype: A Case Study," To be published in *Journal of Aircraft*, Vol. 25, No. 8, Aug. 1988, pp. 724–732.

[3]Horton, H. P., "Laminar Separation Bubbles in Two- and Three-Dimensional Incompressible Flow," Ph.D. Thesis, Univ. of London, UK, 1968.

[4]van Ingen, J. L. and Boermans, L. M. M., "Research on Laminar Separation Bubbles at Delft University of Technology in Relation to Low Reynolds Number Airfoil Aerodynamics," *Proceedings of the Conference on Low Reynolds Number Airfoil Aerodynamics,* University of Notre Dame, June 1985, UN-DAS-CP-77B123, pp. 89–124.

[5]Kwon, O. K. and Pletcher, R. H., "Prediction of Incompressible Separated Boundary Layers Including Viscous-Inviscid Interaction," *Journal of Fluids Engineering,* Vol. 101, Dec. 1979, pp. 466–472.

[6]O'Meara, M. M., "An Experimental Investigation of the Separation Bubble Flowfield Over an Airfoil at Low Reynolds Numbers," Ph.D. Dissertation, Univ. of Notre Dame, IN, 1986.

[7]Brendel, M., "Experimental Study of the Boundary Layer on a Low Reynolds Number Airfoil in Steady and Unsteady Flow," Ph.D. Dissertation, Univ. of Notre Dame, IN, 1986.

[8]Schmidt, G. S., "The Prediction of Transitional Separation Bubbles at Low Reynolds Numbers," Ph.D. Dissertation, Univ. of Notre Dame, IN, 1986.

[9]Mangalam, S. M., Meyers, J. F., Dagenhart, J. R., and Harvey, W. D., "A Study of Laminar Separation Bubble in the Concave Region of an Airfoil Using Laser Velocimetry," Second ASME Laser Velocimetry Symposium, Miami, FL, Nov. 1985.

[10]Brendel, M. and Mueller, T. J., "Boundary-Layer Measurements on an Airfoil at Low Reynolds Numbers," *Journal of Aircraft,* Vol. 25, July 1988, pp. 612–617.

[11]Goldstein, R. J. (ed.), *Fluid Mechanicas Measurements*, Hemisphere, Washington, DC, 1983.

[12]Fitzgerald, E. J., "Experimental Studies of the Transitional Separation Bubble on the NACA 66_3-018 Airfoil at Low Reynolds Numbers," M. S. Thesis, Univ. of Notre Dame, IN, 1988.

[13]Arena, A. V., "An Experimental Investigation of the Leading-Edge Separation Bubble on a Cylindrical Leading-Edge Constant-Thickness Airfoil," M. S. Thesis, Univ. of Notre Dame, IN, 1978.

[14]Schmidt, G. S. and Mueller, T. J., "A Study of the Laminar Separation Bubble on an Airfoil at Low Reynolds Numbers Using Flow-Visualization Techniques," AIAA Paper 87-0242, Jan. 1987.

[15]White, F. M., *Viscous Fluid Flow,* McGraw-Hill, New York, 1974, Chap. 3.

[16]Stewartson, K., "Further Solutions of the Falkner-Skan Equation," *Proceedings of the Cambridge Philosophical Society,* Vol. 50, 1954, pp. 454–465.

[17]Vincent de Paul, M., "Prevision du Decrochage d'un Profil d'Aile en Ecoulement Incompressible," AGARD CP 102, 1972.

[18]Green, J. E., "Two-Dimensional Turbulent Reattachment as a Boundary-Layer Problem," AGARD CP 4, Pt. I, 1966.

Recommended Reading from the AIAA Progress in Astronautics and Aeronautics Series . . . AIAA

Single- and Multi-Phase Flows in an Electromagnetic Field: Energy, Metallurgical and Solar Applications

Herman Branover, Paul S. Lykoudis, and Michael Mond, editors

This text deals with experimental aspects of simple and multi-phase flows applied to power-generation devices. It treats laminar and turbulent flow, two-phase flows in the presence of magnetic fields, MHD power generation, with special attention to solar liquid-metal MHD power generation, MHD problems in fission and fusion reactors, and metallurgical applications. Unique in its interface of theory and practice, the book will particularly aid engineers in power production, nuclear systems, and metallurgical applications. Extensive references supplement the text.

TO ORDER: **Write, Phone, or FAX:** AIAA c/o TASCO, 9 Jay Gould Ct., P.O. Box 753, Waldorf, MD 20604 Phone (301) 645-5643, Dept. 415 ■ FAX (301) 843-0159

Sales Tax: CA residents, 7%; DC, 6%. For shipping and handling add $4.75 for 1–4 books (call for rates for higher quanties). Orders under $50.00 must be prepaid. Foreign orders must be prepaid. Please allow 4 weeks for delivery. Prices are subject to change without notice. Returns will be accepted within 15 days.

1985 762 pp., illus. Hardback
ISBN 0-930403-04-5
AIAA Members $59.95
Nonmembers $89.95
Order Number V-100